Since January 2020 Elsevier has created a COVID-19 resource centre with free information in English and Mandarin on the novel coronavirus COVID-19. The COVID-19 resource centre is hosted on Elsevier Connect, the company's public news and information website.

Analytica Chimica Acta 1229 (2022) 340290

Contents lists available at ScienceDirect

Analytica Chimica Acta

journal homepage: www.elsevier.com/locate/aca

A fast, ultrasensitive SERS immunoassay to detect SARS-CoV-2 in saliva

Moein Mohammadi [a], Delphine Antoine [b], Madison Vitt [a], Julia Marie Dickie [a], Sharmin Sultana Jyoti [a], J. Gerard Wall [b], Patrick A. Johnson [a], Karen E. Wawrousek [a,*]

[a] Chemical Engineering, University of Wyoming, 1000 E. University Ave. Dept. 3295, Laramie, WY, 82071, USA
[b] Microbiology, School of Biological and Chemical Sciences, and SFI Centre for Medical Devices (CÚRAM), University of Galway, Galway H91 TK33, Ireland

HIGHLIGHTS

- We have developed an ultrasensitive SERS assay to detect the SARS-CoV-2 spike protein.
- The assay detects virus at 1.94×10^3 genomes/ml or 4.7 fg mL^{-1} spike protein in saliva.
- SARS-CoV-2 variants of concern, including delta and omicron, are detected.
- Cross-reactivity is not detected with SARS-CoV and MERS-CoV spike protein.
- The single particle assay is stable for at least two weeks in a standard refrigerator.

GRAPHICAL ABSTRACT

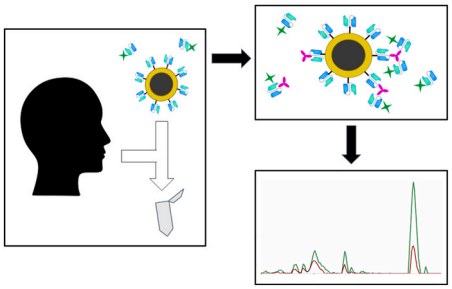

ARTICLE INFO

Keywords:
SARS-CoV-2
COVID-19
Diagnosis
Saliva
Surface-enhanced Raman scattering (SERS)
Single chain variable fragment (scFv)

ABSTRACT

The COVID-19 pandemic has emphasized the need for accurate, rapid, point-of-care diagnostics to control disease transmission. We have developed a simple, ultrasensitive single-particle surface-enhanced Raman spectroscopy (SERS) immunoassay to detect the SARS-CoV-2 spike protein in saliva. This assay relies on the use of single chain Fv (scFv) recombinant antibody expressed in *E. coli* to bind the SARS-CoV-2 spike protein. Recombinant scFv labeled with a SERS-active dye in solution is mixed with unlabeled scFv conjugated to gold-coated magnetic nanoparticles and a sample to be tested. In the presence of the SARS-CoV-2 spike protein, immunocomplexes form and concentrate the labeled scFv close to the gold surface of the nanoparticles, causing an increased SERS signal. The assay detects inactivated SARS-CoV-2 virus and spike protein in saliva at concentrations of 1.94×10^3 genomes mL^{-1} and 4.7 fg mL^{-1}, respectively, making this direct detection antigen test only 2–3 times less sensitive than some qRT-PCR tests. All tested SARS-CoV-2 spike proteins, including those from alpha, beta, gamma, delta, and omicron variants, were detected without recognition of the closely related SARS and MERS spike proteins. This 30 min, no-wash assay requires only mixing, a magnetic separation step, and signal measurements using a hand-held, battery-powered Raman spectrometer, making this assay ideal for ultrasensitive detection of the SARS-CoV-2 virus at the point-of-care.

* Corresponding author.
E-mail address: kwawrous@uwyo.edu (K.E. Wawrousek).

https://doi.org/10.1016/j.aca.2022.340290
Received 2 June 2022; Received in revised form 11 August 2022; Accepted 17 August 2022
Available online 23 August 2022

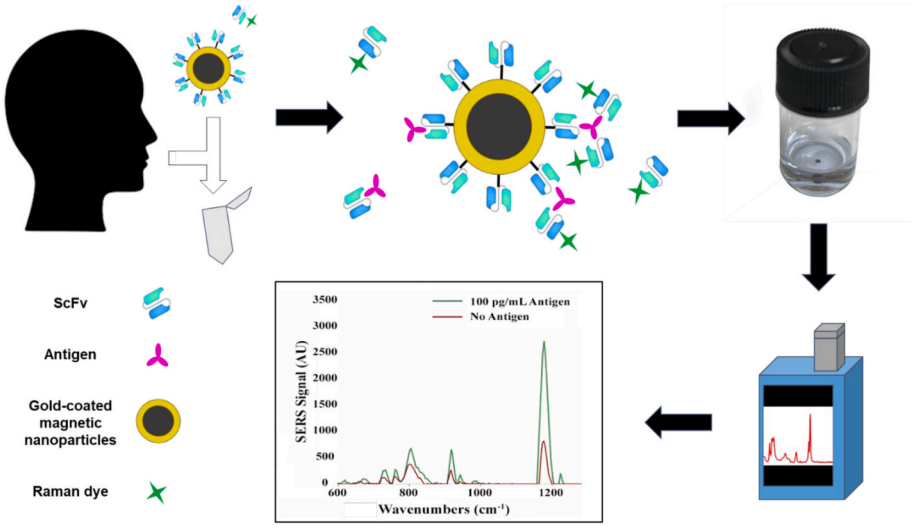

Fig. 1. Schematic of the single-particle SERS immunoassay. Virus-binding scFv antibody fragments labeled with the Raman-active dye malachite green and scFv-conjugated magnetic gold nanoshells are mixed with saliva samples. In the presence of antigen, immunocomplexes form. An external magnet is used to pellet any immunocomplexes, and the SERS spectrum and signal intensity of that pellet is measured. (For interpretation of the references to color in this figure legend, the reader is referred to the Web version of this article.)

1. Introduction

Severe acute respiratory syndrome coronavirus 2 (SARS-CoV-2) virus, which causes the COVID-19 disease, has infected more than 515 million people worldwide and has led to more than 6.25 million fatalities since the outbreak began [1,2]. Caused by mutation of the virus, several SARS-CoV-2 variants have emerged, with the omicron variant arising in late 2021. This highly mutated strain contains more than 60 mutations, with 32 mutations in the spike protein [3]. The omicron variant has been reported to be significantly more transmissible than previous variants of concern (VOCs), while mRNA COVID-19 vaccines protected less against hospitalization with omicron infections than with previous VOCs [4–7].

Early diagnosis of SARS-CoV-2 infection can restrain viral transmission in a population, with pre-symptomatic and asymptomatic individuals responsible for more than 50% of SARS-CoV-2 transmission [8–10]. This can be amplified in the case of omicron infection since a greater proportion of patients are reported to have asymptomatic infections, which may lead to increased transmission [11,12]. One approach to control viral spread is extensive surveillance screening of these pre-symptomatic and asymptomatic populations. qRT-PCR is the most sensitive of the commercially available COVID-19 tests, but the assay is performed in a laboratory and can take several hours to days for an individual to receive the result. Rapid antigen tests using nasal swabs are not meant to replace qRT-PCR but are widely used for symptomatic diagnostic testing and screening for COVID-19. However, compared to laboratory-based molecular tests, they can be less sensitive and have more false-negative results, particularly among asymptomatic people [13,14]. To date, qRT-PCR and rapid tests rely on the use of nasal swabs of the upper respiratory tract or lower nasal swabs [13,15].

Emergence of the omicron variant, with a change in tissue tropism, precipitated the need for altered testing regimes. As compared to earlier VOCs, the omicron variant replicated rapidly in human nasal cells, albeit at lower titres than were eventually found in lung cells [16–19]. Omicron-infected patients have shorter incubation periods prior to symptom onset, and pre-symptomatic viral shedding in saliva has been observed in the absence of nasal shedding [20,21], suggesting an advantage to early viral detection in saliva. Additionally, saliva collection is more comfortable, simple, and can be done by non-professional healthcare workers, thus, more manageable for large-scale screening programs [22,23]. However, saliva samples collected in the early stages of infection can bear low viral loads in the range of 10^3–10^5 copies mL^{-1} [24–26]. As this is below the typical detection limit of 10^5-10^7 genomes mL^{-1} for currently available rapid tests, there is a clear need for ultrasensitive, rapid COVID-19 diagnostic tests [27,28].

Surface-enhanced Raman scattering (SERS) is a robust vibrational spectroscopic technique with various applications, including biological sample identification [29–32]. This technique has previously been utilized to detect low concentrations of viruses, as Raman signals can be enhanced several orders of magnitude (10^7-10^{10}) when using plasmonic nanoparticles and Raman active indicator molecules [33–35]. The availability of hand-held Raman spectrometers makes this sensitive detection method particularly interesting for diagnostic applications, as readings can be taken at the point-of-care.

In the present study, we demonstrate a single-particle SERS immunoassay to detect the spike protein of SARS-CoV-2, as well as the whole SARS-CoV-2 virus, in human saliva. The diagnostic assay utilizes a single-chain variable fragment (scFv), a fusion protein of the heavy and light variable fragments of an antibody, to detect the SARS-CoV-2 spike protein. This scFv was isolated for its ability to bind to the receptor binding domain (RBD) of the SARS-CoV-2 spike protein [35]. An scFv was selected for this study because it can be expressed in *E. coli*, which has a much lower cost than production of whole antibody molecules that are typically raised in animal cells [36,37]. Additionally, the use of an scFv allows a rapid adjustment of the assay if a SARS-CoV-2 variant arises that is no longer recognized because a new scFv can be selected from a library and incorporated into the assay in a matter of weeks. Finally, since the small scFv does not contain the antibody constant domains, the possibility of non-specific binding or cross-reaction with the constant domain is eliminated [38,39].

For the single-particle SERS immunoassay, a saliva sample is incubated with an scFv labeled with a Raman-active dye, as well as scFv conjugated to the surface of gold-coated magnetic nanoparticles (Au@MNP) (Fig. 1). If an immunocomplex forms due to SARS-CoV-2 spike protein in the sample, labeled scFv is brought in close proximity to the scFv-bearing gold surface of the Au@MNP. A magnet is used to concentrate immunocomplexes, and the presence of the Raman-active dye is measured by an increase in SERS signal. SERS signals are measured with a hand-held Raman instrument. The robust assay is compatible with saliva samples, is more sensitive than currently available COVID-19 antigen tests, and has the potential to be used extensively as a point-of-care, rapid diagnostic assay for SARS-CoV-2.

2. Materials and methods

2.1. Materials

All chemicals were purchased from Sigma Aldrich unless otherwise

noted. Delta (B.1.617.2) variant spike trimer (cat. #101147) and gamma (P.1) variant spike trimer (cat. #100989–1) were obtained from BPS Bioscience. The omicron (B.1.1.529) variant spike trimer (cat. #40589-V08H26) was purchased from Sino Biological.

2.2. ScFv3 expression

ScFv3 was isolated from the YamoI library using SARS-CoV-2 spike protein receptor binding domain (RBD) as bait [35]. To optimize scFv3 expression, the pMOD1-*scFv3* plasmid was transformed into *E. coli* HB2151 cells. Overnight cultures of *E. coli* were used to inoculate 50 mL of ZYP-5052 autoinduction broth containing 100 μg mL^{-1} ampicillin. After 48 h growth at 37 °C with shaking, culture supernatants were isolated for protein purification.

2.3. ScFv3 purification

His-tagged scFv3 was purified on a 1 mL Hitrap column (GE Healthcare, UK) loaded with Ni^{2+} and equilibrated with wash buffer (20 mM Na_3PO_4, 0.5 M NaCl, pH 7.4) containing 20 mM imidazole. Prior to loading the column, protein samples were filtered through a 0.4 μm filter, imidazole added to 20 mM, and pH adjusted to 7.4. After sample loading, the column was washed with 20 mL wash buffer containing 20 mM imidazole, 30 mL wash buffer containing 50 mM imidazole, and 10 mL wash buffer containing 80 mM imidazole. ScFv3 was eluted with 400 mM imidazole in wash buffer. Eluted fractions containing scFv3 were dialyzed against phosphate-buffered saline (PBS). Purified protein was visualized on a 12% SDS-PAGE gel stained with Coomassie stain (InstantBlue™, Expedeon, UK), the identity of the protein was confirmed by immunoblot to detect the hexahistidine tag [35], and purified protein was quantified using a BCA assay (Sigma).

2.4. Malachite green labeling

To label purified scFv3 with malachite green, 2 mg of scFv3 was first mixed with 1 mL of 0.1 M sodium bicarbonate buffer (pH 9.0), followed by the addition of 33 μL of a freshly made 10 mg mL^{-1} malachite green isothiocyanate solution in DMSO. The reaction was incubated for 1 h at room temperature (RT) on an orbital shaker, then quenched by the addition of 45 μl freshly prepared 1.5 M hydroxylamine (pH 8.5), shaking for 1 h at RT at 200 RPM. Excess dye was removed using a 0.5 mL 3500 Da MWCO dialysis column (Slide-A-Lyzer MINI dialysis device, cat. #69550, ThermoFisher) using PBS as the dialysis buffer, following the manufacturer's protocol. The successful preparation of MG-scFv3 was confirmed by SDS-PAGE electrophoresis (Supplementary Fig. S1), and the protein was stored at 4 °C in PBS containing 0.05% sodium azide. The amount of malachite green-labeled scFv3 (MG-scFv3) in solution was quantified with the Qubit™ Protein Assay kit (Invitrogen #Q22311) and a Qubit™ 4 Fluorometer. The average concentration of MG-scFv3 was 20 μg mL^{-1}.

2.5. ScFv3 conjugation to Au@MNP

ScFv3 was conjugated to 190 nm magnetic gold nanoshells (Nano-Composix #LBE0272), with a magnetic core diameter of 137 ± 14 nm and calculated surface area of 2.3 m^2/g, as reported by the manufacturer. This size was chosen from the tested 150, 190, and 265 nm particles, as assays using 190 nm particles had a signal/background ratio approximately double that achieved with 150 nm particles and a significantly faster separation time than 265 nm particles. To conjugate protein to the magnetic gold nanoshells (Au@MNP), 10 mg mL^{-1} fresh solutions of 1-ethyl-3-(3-dimethylaminopropyl) carbodiimide (EDC) and sulfo-NHS were made in ultrapure water. Four μL of EDC and 8 μL of sulfo-NHS solutions were mixed with 1 mL of the 190 nm Au@MNP with carboxyl groups on the surface and incubated for 30 min at RT to activate particles. This step makes sulfo-NHS esters on the particle surface that can bind to primary amines present in scFv antibody fragments. Particles were separated from solution using an external magnet and washed once with 5 mM K_3PO_4, 0.5% PEG 20 kDa buffer (pH 7.4). 50 μg of scFv3 was then mixed with 1 mL of activated particles and incubated for 1 h at RT on an orbital shaker at 200 RPM, after which 10 μL of 50% w/v hydroxylamine was added to quench the reaction. After a 10 min incubation, particles were separated via an external magnet, twice washed with 5 mM K_3PO_4, 0.5% PEG 20 kDa buffer (pH 7.4), and resuspended in 1 mL of 0.5X PBS, 0.5% casein, 0.5% bovine serum albumin (BSA), 1% Tween-20, 0.05% sodium azide, pH 8.0. Successful preparation of the scFv3-Au@MNP was confirmed by micro BCA assay (Thermo Scientific), with particle removal prior to spectroscopic measurement, to quantify the amount of protein on the Au@MNP particles. The average amount of scFv3 conjugated to 1.4×10^{10} Au@MNP particles mL^{-1} was 21 μg mL^{-1}.

2.6. Single-particle SERS immunoassay

Immunoassays were performed by mixing 50 μL of scFv3-conjugated magnetic gold nanoshells (scFv3-Au@MNP), 2.5 μL MG-scFv3 (20 μg mL^{-1}), 50 μL of mock sample, and 1X PBS containing 1% BSA to a total volume of 500 μL in a 2 mL glass vial (cat #67502010, Metrohm, Laramie, WY). Mock samples were prepared by spiking human saliva (Innovative Research, MI, cat #IRHUSL50ML) with inactivated SARS-CoV-2 virus or purified spike protein, with subsequent filtration through a 1 μm syringe filter. Assays were incubated on an orbital shaker (200 RPM) at RT for 20 min, with subsequent isolation of immunocomplexes using an external magnet. A portable, handheld Raman spectrometer (Mira DS, Metrohm) was used to quantify the SERS signals of pellets. O-Ring 41 (part #4011953, Danco) was used in the vial holder to focus the 785 nm laser beam on the pellet, allowing the supernatant to be left in the vial for analysis. SERS spectra were measured with raster off, integration time 1 s, laser power 5 (50 mW), and peak height was recorded at 1175 cm^{-1}. All assays were performed in triplicate, and the average of 6 readings was used for each replicate.

2.7. Limit of detection

Signal intensities for limits of detection (LOD) were calculated by $LOD = Y_{blank} + 3 \times SD_{blank}$, where Y_{blank} is the mean of the negative control and SD_{blank} is the standard deviation. The concentration of antigen versus measured SERS intensity was plotted, and the antigen concentration at the LOD was calculated from the Raman intensity using the logarithmic best-fit line. To estimate the limit of detection of a commercially available COVID-19 antigen test (Flowflex), several concentrations of gamma-irradiated Wuhan-Hu-1 SARS-CoV-2 virus were diluted in 80 μL of the manufacturer's supplied buffer and applied to the test according to the manufacturer's protocol.

2.8. Assay stability

SERS assay components were stored at 4 °C, and immunoassays were performed at 1, 7, 10, 14, 21, and 28 days after reagent preparation. SERS signal was measured with no antigen or 50 ng of Wuhan-Hu-1 homotrimeric spike protein. Each assay was performed in triplicate. Reported signal intensities were normalized to the signal intensity of the "No antigen" sample on day 1 to account for minor fluctuations in signal.

3. Results and discussion

3.1. ScFv3 expression

ScFv3 was selected for use in this study because it binds the RBD of the SARS-CoV-2 spike protein and expresses well in *E. coli*. Previously, scFv3 was expressed and purified at moderate yields (2 mg of protein per L of bacterial culture) using a traditional IPTG-induction method [35].

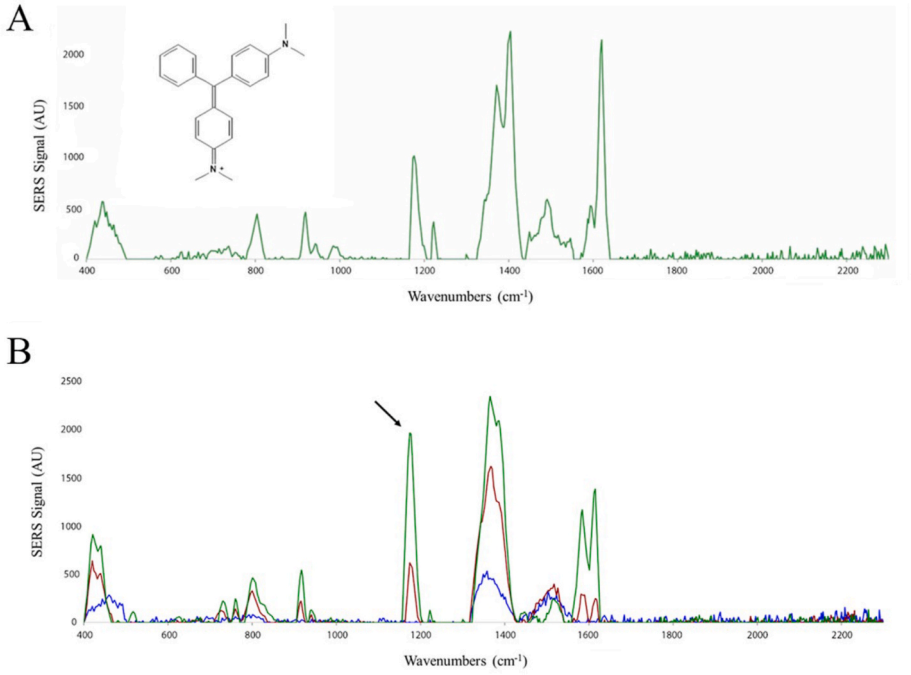

Fig. 2. Malachite green spectra. A) Raman spectrum of a malachite green solution in a glass vial, with (inset) malachite green structure. B) SERS signal from SERS assays containing 50 pg of SARS-CoV-2 omicron trimeric spike protein (green spectrum), a negative control assay with no antigen (red spectrum), and a glass vial containing only reaction buffer (blue spectrum). The arrow indicates the 1175 cm^{-1} peak of malachite green.

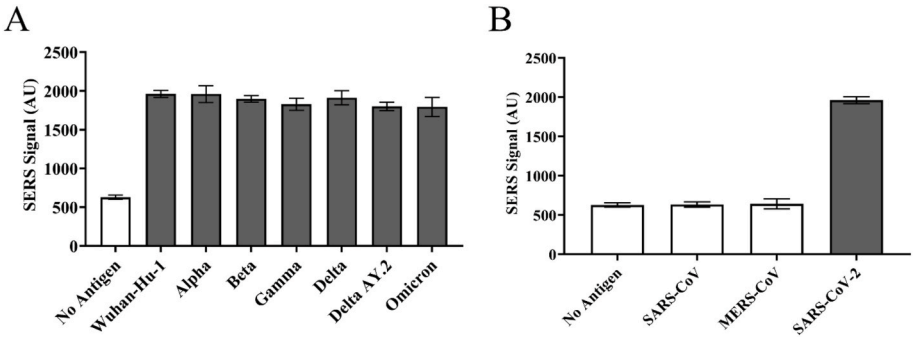

Fig. 3. Assay specificity for SARS-CoV-2 and variants. A) SERS signal at 1175 cm^{-1} of SERS assays containing 50 μl of saliva containing either no antigen or 50 pg SARS-CoV-2 spike homotrimer, B) SERS signal at 1175 cm^{-1} of SERS assays containing 50 μl of saliva with no antigen or 50 pg spike homotrimer of SARS-CoV, MERS-CoV, or SARS-CoV-2 Wuhan-Hu-1 strain. Presented SERS signals are an average of three replicates, with error bars representing the standard deviation. A one-way ANOVA by Dunnett's multiple comparisons test was performed on all samples, and $p < 0.0001$ is indicated by dark gray bars. White bars have no significant difference from the negative control.

To optimize expression, autoinduction of scFv3 expression was carried out at 37 °C, providing several advantages over IPTG induction, including a 2-3-fold higher cell density being attained [40] as well as reduced handling due to the absence of monitoring of cell growth for induction. Using these modifications, consistently high yields of 30–40 mg scFv3 per L of culture were obtained (Supplementary Fig. S2), for a 15 to 20-fold enhancement over previous expression conditions. This higher yield lowers scFv3 production costs, particularly when compared to production costs of full-length antibodies.

3.2. SERS assay validation

A single-particle SERS assay was developed in which scFv3 was directly labeled with the SERS-active dye malachite green (MG-scFv3). The Raman spectrum of malachite green (Fig. 2A) reveals a distinct, single peak at 1175 cm^{-1} that can be used for quantitation of Raman signals. While malachite green does have major peaks at 1175, 1369, and 1618 cm^{-1}, the peak at 1369 cm^{-1} overlaps with the Raman peak from the glass vial used for analysis and the peak at 1618 cm^{-1} is part of at least a doublet of peaks when used in the SERS assay (Fig. 2B). The distinct 1175 cm^{-1} peak of malachite green is due to ring C–H in-plane bending [41].

To test the single-particle SERS assay, scFv3-Au@MNP was incubated with MG-scFv3, Wuhan-Hu-1 SARS-CoV-2 spike homotrimer in saliva, and reaction buffer. Assays containing 50 pg of Wuhan-Hu-1 SARS-CoV-2 spike homotrimer had an average SERS signal of 1961, as compared to 628 of the negative control containing no spike protein, at the 1175 cm^{-1} peak. This clear, significant increase in SERS intensity in the presence of the spike homotrimer indicates that the assay does detect the spike homotrimer (Fig. 3A). The negative control assay, with no antigen present, has a lower malachite green SERS signal associated with it, as there is likely some MG-scFv3 near the Au@MNP pellet giving a non-specific MG SERS signal in this no-wash assay. Additionally, the spike homotrimer is used in this assay, as the spike protein is a homotrimer on the virus surface, and the spike homotrimer has three epitopes to which scFv3 may bind.

The assay was optimized by varying the amount of MG-scFv3 to optimize the signal:background ratio. Briefly, 50 ng of SARS-CoV-2 Wuhan-Hu-1 spike homotrimer in 50 μL saliva was the antigenic sample in a reaction containing 50 μL scFv3-Au@MNP particles (7×10^8 particles), varying amounts of MG-scFv3, and reaction buffer to 500 μL. While the SERS signal increased with increasing amounts of MG-scFv3 in

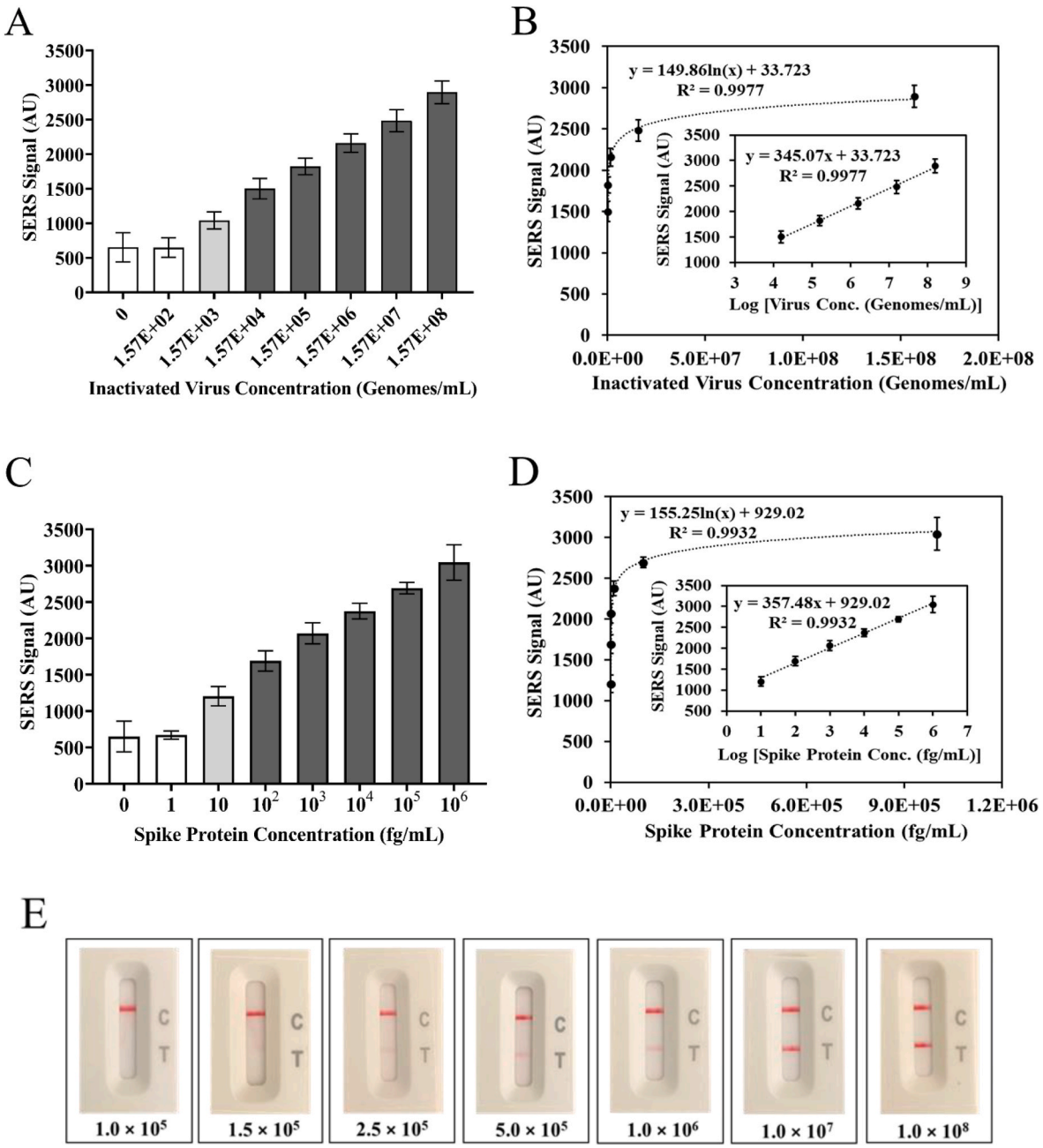

Fig. 4. Limits of detection. Wuhan-Hu-1 SARS-CoV-2 A) gamma-irradiated virus or C) spike homotrimer were tested in the SERS assay by addition of varying concentrations of antigen in saliva. Antigen concentration was plotted against SERS signal (B, D) to calculate antigen concentrations at the limit of detection. Error bars illustrate standard deviation, and signals are reported as an average of three replicates. A one-way ANOVA, followed by Dunnett's multiple comparison test was performed: white bars = no significant difference from negative control; light gray bars: $p = 0.0331$; dark gray bars: $p < 0.0001$. E) a comparable limit of detection for the commercially available Flowflex antigen assay was determined by dilution of gamma-irradiated Wuhan-Hu-1 SARS-CoV-2 virus in 80 μL of the manufacturer's assay solution and application to the lateral flow assay, according to the manufacturer's protocol. Inactivated virus concentrations, reported below each image, are in genomes mL^{-1}.

the reaction, the background signal also increased (Supplementary Fig. S3), likely due to non-specific binding of MG-scFv3 to the scFv3-Au@MNP. The optimal assay contained 7×10^8 scFv3-Au@MNP particles with 1050 ng of scFv3 conjugated to the surface and 50 ng of MG-scFv3 in solution.

Over time, several variants of concern (VOCs) with mutations in the spike protein have emerged [42–44]. The emergence of the delta and omicron variants highlighted how mutated spike proteins may not be recognized well by SARS-CoV-2 antibodies developed to previous strains, as evidenced by the reduction in efficacy of certain monoclonal antibody therapies to the delta, delta AY.2, and omicron strains [45–47]. Since scFv3 was selected by binding of the Wuhan-Hu-1 spike protein receptor binding domain, 50 pg of the alpha (B.1.1.7), beta (B.1.351), gamma (P.1), delta (B.1.617.2), delta AY.2, and omicron (B.1.1.529) variant spike homotrimeric proteins were tested in the SERS immunoassay to ensure scFv3 recognized each variant. Each protein was recognized in the assay with a similar signal intensity to that of the Wuhan-Hu-1 strain (Fig. 3A), indicating scFv3 and the assay recognize SARS-CoV-2 spike protein variants.

The specificity of the assay was tested using the closely related SARS-CoV and MERS-CoV homotrimeric spike proteins. Both SARS-CoV and SARS-CoV-2 are in lineage B of the betacoronavirus genus. The SARS-

CoV-2 genome is 79% identical to that of SARS-CoV, with 76% sequence identity in the spike protein sequence and 74% identity in the RBD region of the spike protein sequence [48]. This high identity is consistent with both SARS-CoV and SARS-CoV-2 gaining cellular entry via the ACE2 receptor, while MERS-CoV enters via the dipeptidyl peptidase 4 receptor [49–51]. MERS-CoV is in lineage C of the betacoronavirus genus, with 50% sequence identity with the SARS-CoV-2 genome [48,52]. Upon addition of 50 pg of SARS-CoV or MERS-CoV homotrimeric spike protein to the assay, there was no significant difference in SERS signal when compared to control samples with no antigen present (Fig. 3B), indicating the assay is highly specific for the SARS-CoV-2 spike protein.

3.3. Limit of detection

The limit of detection of the assay was determined using gamma-irradiated Wuhan-Hu-1 SARS-CoV-2 virus or the Wuhan-Hu-1 SARS-CoV-2 spike homotrimer as antigen. Briefly, varying antigen concentrations were spiked into commercially-available human saliva to create a mock sample, and 50 μL of that mock sample was analyzed in the SERS assay (Fig. 4A, C, Supplementary Fig. S4). Inactivated virus and protein concentrations are reported as those in the mock sample, prior to dilution in the SERS assay. The limit of detection was calculated by the IUPAC standard method ($LOD = Y_{blank} + 3 \times SD_{blank}$, where Y_{blank} is the mean of three negative control replicates and SD_{blank} is the standard deviation) [53–55]. The signal intensity at the LOD was calculated to be 1168 AU. As the SERS signal intensity responds logarithmically to linear changes in concentration, the trendline was used to determine the relationship between signal intensity and concentration (Fig. 4B, D). All data points with a $p < 0.0001$ in ANOVA analysis were included in the trendline. Using the formula of $y = 149.86\ln(x) + 33.723$, where y is the signal intensity and x is the concentration (Fig. 4B), the LOD of the assay was calculated to be 1.94×10^3 genomes mL^{-1}. Using the same approach with the spike homotrimer, where $y = 155.25\ln(x) + 929.02$, the LOD of the spike protein was calculated to be 4.7 fg mL^{-1}. The R^2 of both plots was greater than 0.99, indicating a good trendline fit. While the limit of detection when using purified protein is useful for comparison to other tests reported in the literature, the limit of detection calculated when using inactivated virus is expected to be more clinically relevant.

The sensitivity of this assay was also compared to a commercially available lateral flow rapid antigen assay. Dilutions of gamma-irradiated SARS-CoV-2 were used in the commercially available Flowflex assay to observe the concentration at which the test line, indicating a positive result, is no longer visible (Fig. 4E). The LOD was illustrated to be between 1.5×10^5 and 2.5×10^5 genomes mL^{-1}, indicating the assay is 75 and 130 times less sensitive than the developed SERS immunoassay. While this is less sensitive than the SERS single-particle assay, the SERS single-particle assay also uses a saliva sample, which is not an approved matrix for the Flowflex.

This sensitivity of the SERS assay compares well to other rapid antigen tests, which typically have LODs in the 10^5-10^7 genomes mL^{-1} range for the SARS-CoV-2 virus [27,28] and ng mL^{-1} or pg mL^{-1} detection levels for purified proteins [56–58]. It is also favorable compared to acceptable and desirable LOD thresholds reported in the WHO target product profiles, at 10^6 and 10^4 genomes mL^{-1}, respectively [59]. The rapid antigen test described here would meet the desirable WHO product profile to accurately diagnose individuals with lower levels of viral load, allowing faster identification and potential isolation of emerging cases. In the case of omicron infection, similar or lower viral loads have been reported when compared to that of other VOC infections, suggesting that the high infectiousness of SARS-CoV-2 omicron may be due to factors other than higher viral loads [60,61], thus necessitating the use of sensitive assays for accurate diagnosis.

Nucleic acid amplification tests (NAATs) rely on the amplification of viral sequences to achieve sensitive results, but like antigen tests, sensitivities can vary widely. The limit of detection of a modified CDC assay, the New York SARS-CoV-2 Real-time Reverse Transcriptase (RT)-PCR Diagnostic Panel, was calculated to be 779 ± 27 gene copies mL^{-1}, while the GenMark ePlex qRT-PCR reaction had an experimentally determined limit of detection of 1000 gene copies mL^{-1}, approximately 2.5-fold and 2-fold more sensitive than the SERS assay, respectively. The limits of detection of these qRT-PCR assays were calculated using synthetic RNA diluted in viral transport medium (VTM) to simulate a sample [62], while inactivated virus diluted in saliva was used here to calculate the SERS assay limit of detection. Some qRT-PCR reactions are approved for use with saliva, with reported LODs between 10^2 and 10^4 viral copies mL^{-1} [63,64]. However, these NAATs necessitate specific equipment, training, and can be difficult in resource-constrained environments. False-negative rates of ~30% (range 10–40%) of COVID-19 infected patients have been reported due to inappropriate sampling, stage of infection, improper sample preservation, and technical limits [65–67].

There are point-of-care molecular tests best suited to low to moderate sample volumes, such as the ID NOW COVID-19 test, CovidNudge, and Simplexa Direct assay. The Abbott ID NOW test, an isothermal, qualitative test designed for point-of-care diagnosis, is reported by the manufacturer to have a limit of detection of 125 genome equivalents mL^{-1}, but tested limits of detection reported in the literature vary widely. One study reported an LOD of 262 genomes mL^{-1} when inactivated virus in VTM was used as test material. The study notes that the test may be more likely to give a positive result when samples are stored in VTM, but VTM was removed as an accepted testing matrix due to a concern regarding false negatives [68]. Lephart et al. also note that the assay was less sensitive when using nasal swabs versus nasopharyngeal swabs. A separate study determined an LOD of 64 copies mL^{-1} for this assay, but it is important to note that this is the viral gene copy concentration after dilution in the assay. If that LOD is reported as the viral load of a sample in VTM, the LOD would be 858 copies mL^{-1}. While this is approximately 2.3-fold more sensitive than the SERS assay reported here, the isothermal amplification is carried out one sample at a time in the isothermal amplification and detection equipment, while the SERS assay incubation is done outside of the Raman spectrometer. Therefore, several SERS assays can be conducted in a short amount of time, as each only requires a few seconds in the Raman spectrometer, versus the isothermal, point-of-care NAATs for which samples must be processed and analyzed one at a time.

As the SERS signal depends on the distance between the malachite green and the Au@MNP surface, the signals measured with purified spike homotrimer and inactivated virus were compared. The LOD concentration of 1.94×10^3 genomes mL^{-1} obtained with inactivated Wuhan-Hu-1 SARS-CoV-2 virus is equivalent to 14.9–55.8 fg mL^{-1} of purified spike protein, assuming 26 ± 15 spike homotrimers per SARS-CoV-2 virion [69] and one genome copy per virion. Therefore, the LOD when using inactivated virus is approximately 3–12 times higher than the LOD calculated for the purified spike protein. This difference may be due to the design of the assay, in which MG-scFv3 bound to a virus may be physically farther from the scFv3-Au@MNP surface than when MG-scFv3 binds the spike homotrimer, potentially causing a weaker SERS signal. It is also possible that epitopes on the spike protein might not be fully accessible in the inactivated virus structure. Despite this difference, the assay is sufficiently sensitive to detect concentrations of SARS-CoV-2 that would produce a false negative result in other rapid diagnostic assays.

3.4. Assay stability

To determine the stability of the assay reagents at 4 °C, MG-scFv3 and scFv3-Au@MNP were stored in a standard refrigerator for 28 days. At 1, 7, 10, 14, 21, and 28 days, aliquots of each reagent were used in a SERS assay with 50 ng of SARS-CoV-2 Wuhan-Hu-1 spike homotrimer as antigen. No drop in signal was observed upon reagent storage

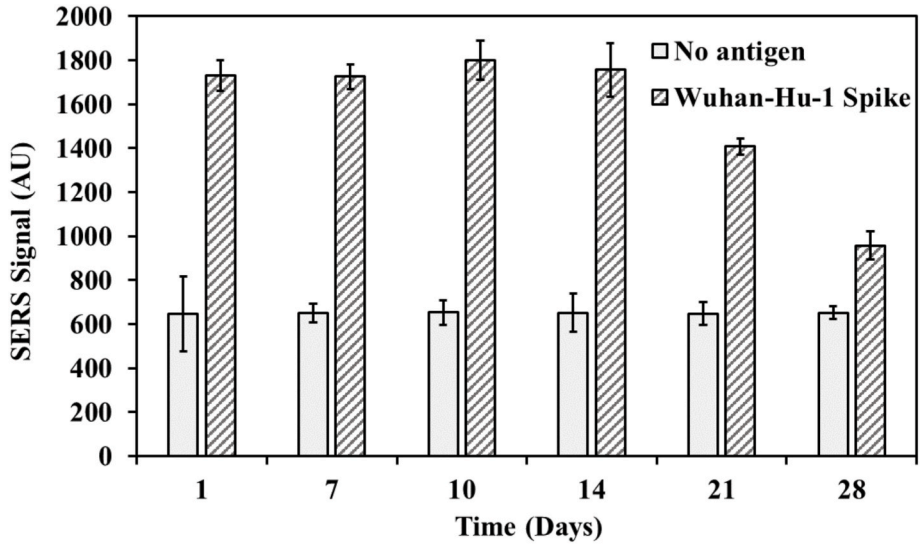

Fig. 5. Stability of assay reagents. No antigen or 50 μl of saliva containing 50 ng SARS-CoV-2 Wuhan-Hu-1 spike homotrimer was added to SERS assay. SERS signal was assessed after 1, 7, 10, 14, 21, and 28 days of reagent storage at 4 °C. All SERS signals were normalized with respect to the signal intensity of the "No antigen" sample on day 1.

for two weeks at 4 °C, and the assay was still functional after three weeks of reagent storage in the refrigerator (Fig. 5). These reagents were significantly more stable than those used in a previous two particle SERS assay to detect SARS-CoV-2, in which assay components degraded to the point that the assay was non-functional within 7 days when stored at 4 °C (data not shown).

4. Conclusions

We report the development of an ultrasensitive, rapid SARS-CoV-2 diagnostic using a hand-held Raman spectrometer for signal detection. The immunoassay relies on the use of a highly expressed scFv, for which expression was optimized for yields of 30–40 mg of purified protein per L of *E. coli* culture. The assay detects all tested SARS-CoV-2 variant of concern spike proteins, including that from the omicron strain, without recognizing the closely related SARS-CoV and MERS-CoV spike proteins, indicating the assay is specific for SARS-CoV-2. The assay detects inactivated SARS-CoV-2 at concentrations of 1.94×10^3 genomes mL^{-1}, and purified spike homotrimer at 4.7 fg mL^{-1}, in saliva, making it ideal for testing of the omicron strain, which can be present in saliva before nasal swabs [20]. This 30 min, no-wash assay is significantly more sensitive than currently available rapid lateral flow tests for COVID-19 detection, potentially allowing the detection of SARS-CoV-2 infection in pre-symptomatic or asymptomatic individuals through this rapid test. This assay can be used in healthcare settings, as well as workplaces, schools, airports, etc., where large-scale screening is needed to reduce transmission and manage the COVID-19 pandemic.

CRediT authorship contribution statement

Moein Mohammadi: Investigation, Validation, Visualization, Writing – original draft, Writing – review & editing. **Delphine Antoine:** Investigation, Visualization, Writing – original draft, Writing – review & editing. **Madison Vitt:** Investigation, Validation. **Julia Marie Dickie:** Investigation, Visualization, Writing – review & editing. **Sharmin Sultana Jyoti:** Investigation. **J. Gerard Wall:** Conceptualization, Project administration, Supervision, Funding acquisition, Writing – original draft, Writing – review & editing. **Patrick A. Johnson:** Conceptualization, Project administration, Supervision, Funding acquisition, Writing – review & editing. **Karen E. Wawrousek:** Conceptualization, Project administration, Supervision, Funding acquisition, Writing – original draft, Writing – review & editing.

Declaration of competing interest

The authors declare that they have no known competing financial interests or personal relationships that could have appeared to influence the work reported in this paper.

Data availability

Data will be made available on request.

5. Acknowledgements

The authors thank Noah Hull and Cari Sloma for helpful discussions, and Ahmad Ansari for technical assistance. This work was supported by the Health Research Board, Ireland COVID-19 Pandemic Rapid Response Funding Opportunity 2020 (grant no. COV19-2020-081) and funds granted from CARES Act Covid Innovation Fund. The following reagents were obtained through BEI Resources, NIAID, NIH: Spike Glycoprotein (Stabilized) from SARS-CoV-2, Wuhan-Hu-1 with C-Terminal Histidine and Twin-strep Tags, Recombinant from HEK293 Cells, NR-53589; Spike Glycoprotein (Stabilized) from SARS-CoV-2, B.1.1.7 Lineage with C-Terminal Histidine and Avi Tags, Recombinant from HEK293 Cells, NR-55311; Spike Glycoprotein (Stabilized) from SARS-CoV-2, B.1.351 Lineage with C-Terminal Histidine and Avi Tags, Recombinant from HEK293 Cells, NR-55310; Spike Glycoprotein (Stabilized) from SARS-CoV-2, AY.2 Lineage (Delta variant) with C-Terminal Histidine and Avi Tags, Recombinant from HEK293 Cells, NR-55711; Spike Glycoprotein (Stabilized) from MERS Coronavirus, England-1 with C-Terminal Histidine and Twin-strep Tags, Recombinant from HEK293 Cells, NR-53591; Spike Glycoprotein (Stabilized) from SARS Coronavirus, Tor2 with C-Terminal Histidine and Strep II Tags, Recombinant from HEK293 Cells, NR-53590; SARS-CoV-2, Isolate USA-WA1/2020, Gamma-irradiated, NR-52287, contributed by the Centers for Disease Control and Prevention.

Appendix A. Supplementary data

Supplementary data to this article can be found online at https://doi.org/10.1016/j.aca.2022.340290.

References

[1] World Health Organization, WHO coronavirus (COVID-19) dashboard. https://covid19.who.int. (Accessed 25 May 2022).

[2] COVID-19 Map, Johns hopkins coronavirus resource center. https://coronavirus.jhu.edu/map.html. (Accessed 25 May 2022).

[3] C. Nie, A.K. Sahoo, R.R. Netz, A. Herrmann, M. Ballauff, R. Haag, Charge matters: mutations in omicron variant favor binding to cells, Chembiochem 23 (2022), e202100681, https://doi.org/10.1002/cbic.202100681.

[4] K.P.Y. Hui, J.C.W. Ho, M. Cheung, K. Ng, R.H.H. Ching, K. Lai, T.T. Kam, H. Gu, K.-Y. Sit, M.K.Y. Hsin, T.W.K. Au, L.L.M. Poon, M. Peiris, J.M. Nicholls, M.C.W. Chan, SARS-CoV-2 Omicron variant replication in human bronchus and lung ex vivo, Nature 603 (2022) 715–720, https://doi.org/10.1038/s41586-022-04479-6.

[5] B.J. Willett, J. Grove, O.A. MacLean, C. Wilkie, N. Logan, G.D. Lorenzo, W. Furnon, S. Scott, M. Manali, A. Szemiel, S. Ashraf, E. Vink, W.T. Harvey, C. Davis, R. Orton, J. Hughes, P. Holland, V. Silva, D. Pascall, K. Puxty, A. da S. Filipe, G. Yebra, S. Shaaban, M.T.G. Holden, R.M. Pinto, R. Gunson, K. Templeton, P.R. Murcia, A. H. Patel, J. Haughney, D.L. Robertson, M. Palmarini, S. Ray, E.C. Thomson, T.C.-19 G.U., COG-U. Consortium, SARS-CoV-2 Omicron is an immune escape variant with an altered cell entry pathway, Nature Microbiology 7 (2022) 1161–1179, https://doi.org/10.1038/s41564-022-01143-7.

[6] A. Wilhelm, M. Widera, K. Grikscheit, T. Toptan, B. Schenk, C. Pallas, M. Metzler, N. Kohmer, S. Hoehl, F.A. Helfritz, T. Wolf, U. Goetsch, S. Ciesek, Reduced neutralization of SARS-CoV-2 omicron variant by vaccine sera and monoclonal antibodies, medRxiv (2021), https://doi.org/10.1101/2021.12.07.21267432.

[7] A.S. Lauring, M.W. Tenforde, J.D. Chappell, M. Gaglani, A.A. Ginde, T. McNeal, S. Ghamande, D.J. Douin, H.K. Talbot, J.D. Casey, N.M. Mohr, A. Zepeski, N. I. Shapiro, K.W. Gibbs, D.C. Files, D.N. Hager, A. Shehu, M.E. Prekker, H. L. Erickson, M.C. Exline, M.N. Gong, A. Mohamed, N.J. Johnson, V. Srinivasan, J. S. Steingrub, I.D. Peltan, S.M. Brown, E.T. Martin, A.S. Monto, A. Khan, C. L. Hough, L.W. Busse, C.C. ten Lohuis, A. Duggal, J.G. Wilson, A.J. Gordon, N. Qadir, S.Y. Chang, C. Mallow, C. Rivas, H.M. Babcock, J.H. Kwon, N. Halasa, C. G. Grijalva, T.W. Rice, W.B. Stubblefield, A. Baughman, K.N. Womack, J.P. Rhoads, C.J. Lindsell, K.W. Hart, Y. Zhu, K. Adams, S.J. Schrag, S.M. Olson, M. Kobayashi, J.R. Verani, M.M. Patel, W.H. Self, Clinical severity of, and effectiveness of mRNA vaccines against, covid-19 from omicron, delta, and alpha SARS-CoV-2 variants in the United States: prospective observational study, BMJ 376 (2022), e069761, https://doi.org/10.1136/bmj-2021-069761.

[8] M.A. Johansson, T.M. Quandelacy, S. Kada, P.V. Prasad, M. Steele, J.T. Brooks, R. B. Slayton, M. Biggerstaff, J.C. Butler, SARS-CoV-2 transmission from people without COVID-19 symptoms, JAMA Netw. Open 4 (2021), e2035057, https://doi.org/10.1001/jamanetworkopen.2020.35057.

[9] N. Sugano, W. Ando, W. Fukushima, Cluster of severe acute respiratory syndrome coronavirus 2 infections linked to music clubs in osaka, Japan, J. Infect. Dis. 222 (2020) 1635–1640, https://doi.org/10.1093/infdis/jiaa542.

[10] C. Yang, S. Zhang, S. Lu, J. Yang, Y. Cheng, Y. Liu, L. Zhao, J. Gong, J. Xu, All five COVID-19 outbreaks during epidemic period of 2020/2021 in China were instigated by asymptomatic or pre-symptomatic individuals, J. Biosaf. Biosecurity. 3 (2021) 35–40, https://doi.org/10.1016/j.jobb.2021.04.001.

[11] C.J.L. Murray, COVID-19 will continue but the end of the pandemic is near, Lancet 399 (2022) 417–419, https://doi.org/10.1016/S0140-6736(22)00100-3.

[12] N. Garrett, A. Tapley, J. Andriesen, I. Seocharan, L.H. Fisher, L. Bunts, N. Espy, C. L. Wallis, A.K. Randhawa, N. Ketter, M. Yacovone, A. Goga, L.-G. Bekker, G. E. Gray, L. Corey, High rate of asymptomatic carriage associated with variant strain omicron, medRxiv (2022), https://doi.org/10.1101/2021.12.20.21268130.

[13] World Health Organization, Recommendations for national SARS-CoV-2 testing strategies and diagnostic capacities. https://www.who.int/publications-detail-redirect/WHO-2019-nCoV-lab-testing-2021.1-eng. (Accessed 26 May 2022).

[14] Centers for Disease Control and Prevention, Guidance for antigen testing for SARS-CoV-2 for healthcare providers testing individuals in the community. https://www.cdc.gov/coronavirus/2019-ncov/lab/resources/antigen-tests-guidelines.html, 2020. (Accessed 25 May 2022).

[15] Centers for Disease Control and Prevention, Interim guidelines for collecting and handling of clinical specimens for COVID-19 testing. https://www.cdc.gov/coronavirus/2019-ncov/lab/guidelines-clinical-specimens.html, 2020. (Accessed 25 May 2022).

[16] T.P. Peacock, J.C. Brown, J. Zhou, N. Thakur, K. Sukhova, J. Newman, R. Kugathasan, A.W.C. Yan, W. Furnon, G.D. Lorenzo, V.M. Cowton, D. Reuss, M. Moshe, J.L. Quantrill, O.K. Platt, M. Kaforou, A.H. Patel, M. Palmarini, D. Bailey, W.S. Barclay, The altered entry pathway and antigenic distance of the SARS-CoV-2 Omicron variant map to separate domains of spike protein, bioRxiv (2022), https://doi.org/10.1101/2021.12.31.474653.

[17] G. Marais, N. Hsiao, A. Iranzadeh, D. Doolabh, R. Joseph, A. Enoch, C. Chu, C. Williamson, A. Brink, D. Hardie, Improved oral detection is a characteristic of Omicron infection and has implications for clinical sampling and tissue tropism, J. Clin. Virol. 152 (2022), 105170, https://doi.org/10.1016/j.jcv.2022.105170.

[18] G. Marais, N. Hsiao, A. Iranzadeh, D. Doolabh, A. Enoch, C. Chu, C. Williamson, A. Brink, D. Hardie, Saliva swabs are the preferred sample for Omicron detection, medRxiv (2021), https://doi.org/10.1101/2021.12.22.21268246.

[19] K.-D. Vihta, K.B. Pouwels, T.E.A. Peto, E. Pritchard, T. House, R. Studley, E. Rourke, D. Cook, I. Diamond, D. Crook, D.A. Clifton, P.C. Matthews, N. Stoesser, D.W. Eyre, A.S. Walker, the C.-19 I.S. Team, Omicron-Associated Changes in Severe Acute Respiratory Syndrome Coronavirus 2 (SARS-CoV-2) Symptoms in the United Kingdom, Clinical Infectious Diseases ciac613 (2022), https://doi.org/10.1093/cid/ciac613.

[20] B. Adamson, R. Sikka, A.L. Wyllie, P. Premsrirut, Discordant SARS-CoV-2 PCR and rapid antigen test results when infectious: a december 2021 occupational case series, medRxiv (2022), https://doi.org/10.1101/2022.01.04.22268770.

[21] R. Ke, C. Zitzmann, D.D. Ho, R.M. Ribeiro, A.S. Perelson, In vivo kinetics of SARS-CoV-2 infection and its relationship with a person's infectiousness, Proc. Natl. Acad. Sci. USA 118 (2021), e2111477118, https://doi.org/10.1073/pnas.2111477118.

[22] I. Yokota, P.Y. Shane, T. Teshima, Logistic advantage of two-step screening strategy for SARS-CoV-2 at airport quarantine, Travel Med, Inf. Disp. 43 (2021), 102127, https://doi.org/10.1016/j.tmaid.2021.102127.

[23] M. Huber, P.W. Schreiber, T. Scheier, A. Audigé, R. Buonomano, A. Rudiger, D. L. Braun, G. Eich, D.I. Keller, B. Hasse, J. Böni, C. Berger, H.F. Günthard, A. Manrique, A. Trkola, High efficacy of saliva in detecting SARS-CoV-2 by RT-PCR in adults and children, Microorganisms 9 (2021) 642, https://doi.org/10.3390/microorganisms9030642.

[24] A. Winnett, M.M. Cooper, N. Shelby, A.E. Romano, J.A. Reyes, J. Ji, M.K. Porter, E. S. Savela, J.T. Barlow, R. Akana, C. Tognazzini, M. Feaster, Y. Goh, R.F. Ismagilov, SARS-CoV-2 viral load in saliva rises gradually and to moderate levels in some humans, medRxiv (2020), https://doi.org/10.1101/2020.12.09.20239467.

[25] S. Kissler, J.R. Fauver, C. Mack, C.G. Tai, M.I. Breban, A.E. Watkins, R.M. Samant, D.J. Anderson, D.D. Ho, N.D. Grubaugh, Y. Grad, Densely sampled viral trajectories suggest longer duration of acute infection with B.1.1.7 variant relative to non-B.1.1.7 SARS-CoV-2. https://dash.harvard.edu/handle/1/37366884, 2021. (Accessed 25 May 2022).

[26] S.M. Kissler, J.R. Fauver, C. Mack, S.W. Olesen, C. Tai, K.Y. Shiue, C. Kalinich, S. Jednak, I. Ott, C. Vogels, J. Wohlgemuth, J. Weisberger, J. DiFiori, D. J. Anderson, J. Mancell, D. Ho, N.D. Grubaugh, Y.H. Grad, Viral dynamics of SARS-CoV-2 infection and the predictive value of repeat testing, medRxiv (2020), https://doi.org/10.1101/2020.10.21.20217042.

[27] A.I. Cubas-Atienzar, K. Kontogianni, T. Edwards, D. Wooding, K. Buist, C. R. Thompson, C.T. Williams, E.I. Patterson, G.L. Hughes, L. Baldwin, C. Escadafal, J.A. Sacks, E.R. Adams, Limit of detection in different matrices of 19 commercially available rapid antigen tests for the detection of SARS-CoV-2, Sci. Rep. 11 (2021), 18313, https://doi.org/10.1038/s41598-021-97489-9.

[28] S. Stanley, D.J. Hamel, I.D. Wolf, S. Riedel, S. Dutta, A. Cheng, J.E. Kirby, P. J. Kanki, Limit of detection for rapid antigen testing of the SARS-CoV-2 omicron variant, medRxiv (2022), https://doi.org/10.1101/2022.01.28.22269968.

[29] H. Chen, A. Das, L. Bi, N. Choi, J.-I. Moon, Y. Wu, S. Park, J. Choo, Recent advances in surface-enhanced Raman scattering-based microdevices for point-of-care diagnosis of viruses and bacteria, Nanoscale 12 (2020) 21560–21570, https://doi.org/10.1039/D0NR06340A.

[30] J.J.S. Rickard, V. Di-Pietro, D.J. Smith, D.J. Davies, A. Belli, P.G. Oppenheimer, Rapid optofluidic detection of biomarkers for traumatic brain injury via surface-enhanced Raman spectroscopy, Nat. Biomed. Eng. 4 (2020) 610–623, https://doi.org/10.1038/s41551-019-0510-4.

[31] L.F. Tadesse, F. Safir, C.-S. Ho, X. Hasbach, B. (Pierre) Khuri-Yakub, S.S. Jeffrey, A. A.E. Saleh, J. Dionne, Toward rapid infectious disease diagnosis with advances in surface-enhanced Raman spectroscopy, J. Chem. Phys. 152 (2020), 240902, https://doi.org/10.1063/1.5142767.

[32] A. Chakraborty, A. Ghosh, A. Barui, Advances in surface-enhanced Raman spectroscopy for cancer diagnosis and staging, J. Raman Spectrosc. 51 (2020) 7–36, https://doi.org/10.1002/jrs.5726.

[33] E.J. Blackie, E.C. Le Ru, P.G. Etchegoin, Single-molecule surface-enhanced Raman spectroscopy of nonresonant molecules, J. Am. Chem. Soc. 131 (2009) 14466–14472, https://doi.org/10.1021/ja905319w.

[34] E.C. Le Ru, E. Blackie, M. Meyer, P.G. Etchegoin, Surface enhanced Raman scattering enhancement factors: a comprehensive study, J. Phys. Chem. C 111 (2007) 13794–13803, https://doi.org/10.1021/jp0687908.

[35] D. Antoine, M. Mohammadi, M. Vitt, J.M. Dickie, S.S. Jyoti, M.A. Tilbury, P. A. Johnson, K.E. Wawrousek, J.G. Wall, Rapid, point-of-care scFv-SERS assay for femtogram level detection of SARS-CoV-2, ACS Sens. 7 (2022) 866–873, https://doi.org/10.1021/acssensors.1c02664.

[36] V. Joosten, C. Lokman, C.A. van den Hondel, P.J. Punt, The production of antibody fragments and antibody fusion proteins by yeasts and filamentous fungi, Microb. Cell Factories 2 (2003) 1, https://doi.org/10.1186/1475-2859-2-1.

[37] S.K. Gupta, P. Shukla, Microbial platform technology for recombinant antibody fragment production: a review, Crit. Rev. Microbiol. 43 (2017) 31–42, https://doi.org/10.3109/1040841X.2016.1150959.

[38] P.P. Monnier, R.J. Vigouroux, N.G. Tassew, In vivo applications of single chain Fv (variable domain) (scFv) fragments, Antibodies 2 (2013) 193–208, https://doi.org/10.3390/antib2020193.

[39] M. Johnson, Antibody structure and antibody fragments, Mater. Methods. (2022), https://doi.org/10.13070/mm.en.3.160.

[40] F.W. Studier, Protein production by auto-induction in high-density shaking cultures, Protein Expr, Purif 41 (2005) 207–234, https://doi.org/10.1016/j.pep.2005.01.016.

[41] K. Lai, Y. Zhang, R. Du, F. Zhai, B.A. Rasco, Y. Huang, Determination of chloramphenicol and crystal violet with surface enhanced Raman spectroscopy, Sens. Instrum. Food Qual. Saf. 5 (2011) 19–24, https://doi.org/10.1007/s11694-011-9106-8.

[42] R.P. Walensky, H.T. Walke, A.S. Fauci, SARS-CoV-2 variants of concern in the United States—challenges and opportunities, JAMA 325 (2021) 1037–1038, https://doi.org/10.1001/jama.2021.2294.

[43] S.S. Abdool Karim, T. de Oliveira, New SARS-CoV-2 variants — clinical, public Health, and vaccine implications, N. Engl. J. Med. 384 (2021) 1866–1868, https://doi.org/10.1056/NEJMc2100362.

[44] D. Tian, Y. Sun, H. Xu, Q. Ye, The emergence and epidemic characteristics of the highly mutated SARS-CoV-2 Omicron variant, J. Med. Virol. 94 (2022) 2376–2383, https://doi.org/10.1002/jmv.27643.
[45] U.S. FOOD & DRUG ADMINISTRATION, Fact sheet for Health care providers emergency use authorization (eua) of bamlanivimab and etesevimab 01242022. https://www.fda.gov/media/145802/download. (Accessed 25 May 2022).
[46] U.S. FOOD & DRUG ADMINISTRATION, Coronavirus (COVID-19) update: FDA limits use of certain monoclonal antibodies to treat COVID-19 due to the omicron variant. https://www.fda.gov/news-events/press-announcements/coronavirus-covid-19-update-fda-limits-use-certain-monoclonal-antibodies-treat-covid-19-due-omicron, 2022. (Accessed 25 May 2022).
[47] U.S. FOOD & DRUG ADMINISTRATION, Fact sheet for Health care providers emergency use authorization (eua) of REGEN-COV® (casirivimab and imdevimab). https://www.fda.gov/media/145611/download. (Accessed 25 May 2022).
[48] J.A. Jaimes, N.M. André, J.S. Chappie, J.K. Millet, G.R. Whittaker, Phylogenetic analysis and structural modeling of SARS-CoV-2 spike protein reveals an evolutionary distinct and proteolytically sensitive activation loop, J. Mol. Biol. 432 (2020) 3309–3325, https://doi.org/10.1016/j.jmb.2020.04.009.
[49] M. Hoffmann, H. Kleine-Weber, S. Schroeder, N. Krüger, T. Herrler, S. Erichsen, T. S. Schiergens, G. Herrler, N.-H. Wu, A. Nitsche, M.A. Müller, C. Drosten, S. Pöhlmann, SARS-CoV-2 cell entry depends on ACE2 and TMPRSS2 and is blocked by a clinically proven protease inhibitor, Cell 181 (2020) 271–280, https://doi.org/10.1016/j.cell.2020.02.052, e8.
[50] D. Blanco-Melo, B.E. Nilsson-Payant, W.-C. Liu, S. Uhl, D. Hoagland, R. Møller, T. X. Jordan, K. Oishi, M. Panis, D. Sachs, T.T. Wang, R.E. Schwartz, J.K. Lim, R. A. Albrecht, B.R. tenOever, Imbalanced host response to SARS-CoV-2 drives development of COVID-19, Cell 181 (2020) 1036–1045, https://doi.org/10.1016/j.cell.2020.04.026, e9.
[51] P. Zhou, X.-L. Yang, X.-G. Wang, B. Hu, L. Zhang, W. Zhang, H.-R. Si, Y. Zhu, B. Li, C.-L. Huang, H.-D. Chen, J. Chen, Y. Luo, H. Guo, R.-D. Jiang, M.-Q. Liu, Y. Chen, X.-R. Shen, X. Wang, X.-S. Zheng, K. Zhao, Q.-J. Chen, F. Deng, L.-L. Liu, B. Yan, F.-X. Zhan, Y.-Y. Wang, G.-F. Xiao, Z.-L. Shi, A pneumonia outbreak associated with a new coronavirus of probable bat origin, Nature 579 (2020) 270–273, https://doi.org/10.1038/s41586-020-2012-7.
[52] R. Lu, X. Zhao, J. Li, P. Niu, B. Yang, H. Wu, W. Wang, H. Song, B. Huang, N. Zhu, Y. Bi, X. Ma, F. Zhan, L. Wang, T. Hu, H. Zhou, Z. Hu, W. Zhou, L. Zhao, J. Chen, Y. Meng, J. Wang, Y. Lin, J. Yuan, Z. Xie, J. Ma, W.J. Liu, D. Wang, W. Xu, E. C. Holmes, G.F. Gao, G. Wu, W. Chen, W. Shi, W. Tan, Genomic characterisation and epidemiology of 2019 novel coronavirus: implications for virus origins and receptor binding, Lancet 395 (2020) 565–574, https://doi.org/10.1016/S0140-6736(20)30251-8.
[53] C. Wang, R. Xiao, S. Wang, X. Yang, Z. Bai, X. Li, Z. Rong, B. Shen, S. Wang, Magnetic quantum dot based lateral flow assay biosensor for multiplex and sensitive detection of protein toxins in food samples, Biosens. Bioelectron. 146 (2019), 111754, https://doi.org/10.1016/j.bios.2019.111754.
[54] J. Hu, Y.-Z. Jiang, L.-L. Wu, Z. Wu, Y. Bi, G. Wong, X. Qiu, J. Chen, D.-W. Pang, Z.-L. Zhang, Dual-signal readout nanospheres for rapid point-of-care detection of ebola virus Glycoprotein, Anal. Chem. 89 (2017) 13105–13111, https://doi.org/10.1021/acs.analchem.7b02222.
[55] X. Wang, N. Choi, Z. Cheng, J. Ko, L. Chen, J. Choo, Simultaneous detection of dual nucleic acids using a SERS-based lateral flow assay biosensor, Anal. Chem. 89 (2017) 1163–1169, https://doi.org/10.1021/acs.analchem.6b03536.
[56] L. Fabiani, M. Saroglia, G. Galatà, R. De Santis, S. Fillo, V. Luca, G. Faggioni, N. D'Amore, E. Regalbuto, P. Salvatori, G. Terova, D. Moscone, F. Lista, F. Arduini, Magnetic beads combined with carbon black-based screen-printed electrodes for COVID-19: a reliable and miniaturized electrochemical immunosensor for SARS-CoV-2 detection in saliva, Biosens. Bioelectron. 171 (2021), 112686, https://doi.org/10.1016/j.bios.2020.112686.
[57] B.D. Grant, C.E. Anderson, J.R. Williford, L.F. Alonzo, V.A. Glukhova, D.S. Boyle, B. H. Weigl, K.P. Nichols, SARS-CoV-2 coronavirus nucleocapsid antigen-detecting half-strip lateral flow assay toward the development of point of care tests using commercially available reagents, Anal. Chem. 92 (2020) 11305–11309, https://doi.org/10.1021/acs.analchem.0c01975.
[58] D. Liu, C. Ju, C. Han, R. Shi, X. Chen, D. Duan, J. Yan, X. Yan, Nanozyme chemiluminescence paper test for rapid and sensitive detection of SARS-CoV-2 antigen, Biosens. Bioelectron. 173 (2020), 112817, https://doi.org/10.1016/j.bios.2020.112817.
[59] World Health Organization, COVID-19 Target product profiles for priority diagnostics to support response to the COVID-19 pandemic v.1.0. https://www.who.int/publications/m/item/covid-19-target-product-profiles-for-priority-diagnostics-to-support-response-to-the-covid-19-pandemic-v.0.1, 2020. (Accessed 25 May 2022).
[60] A. Fall, R.E. Eldesouki, J. Sachithanandham, C.P. Morris, J.M. Norton, D.C. Gaston, M. Forman, O. Abdullah, N. Gallagher, M. Li, N.J. Swanson, A. Pekosz, E.Y. Klein, H.H. Mostafa, The displacement of the SARS-CoV-2 variant Delta with Omicron: an investigation of hospital admissions and upper respiratory viral loads, EBioMedicine 79 (2022), 104008, https://doi.org/10.1016/j.ebiom.2022.104008.
[61] O. Puhach, K. Adea, N. Hulo, P. Sattonnet, C. Genecand, A. Iten, F.J. Bausch, L. Kaiser, P. Vetter, I. Eckerle, B. Meyer, Infectious viral load in unvaccinated and vaccinated individuals infected with ancestral, Delta or Omicron SARS-CoV-2, Nat. Med. 28 (2022) 1491–1500, https://doi.org/10.1038/s41591-022-01816-0.
[62] W. Zhen, R. Manji, E. Smith, G.J. Berry, Comparison of four molecular in vitro diagnostic assays for the detection of SARS-CoV-2 in nasopharyngeal specimens, J. Clin. Microbiol. 58 (2020), https://doi.org/10.1128/JCM.00743-20 e00743-20.
[63] Q. Sun, J. Li, H. Ren, L. Pastor, Y. Loginova, R. Madej, K. Taylor, J.K. Wong, Z. Zhang, A. Zhang, C.M. Lu, M.Y. Sha, Saliva as a testing specimen with or without pooling for SARS-CoV-2 detection by multiplex RT-PCR test, PLoS One 16 (2021), e0243183, https://doi.org/10.1371/journal.pone.0243183.
[64] S. Pijuan-Galito, F.S. Tarantini, H. Tomlin, H. Jenkins, J.L. Thompson, D. Scales, A. Stroud, A. Tellechea Lopez, J. Hassall, P.G. McTernan, A. Coultas, A. Arendt-Tranholm, C. Reffin, I. Hill, I. Lee, S. Wu, J. Porte, J. Chappell, K. Lis-Slimak, K. Kaneko, L. Doolan, M. Ward, M. Stonebridge, M. Ilyas, P. McClure, P. Tighe, P. Gwynne, R. Hyde, J. Ball, C. Seedhouse, A.V. Benest, M. Petrie, C. Denning, Saliva for COVID-19 testing: simple but useless or an undervalued resource? Front. Virol. 1 (2021) https://doi.org/10.3389/fviro.2021.778790.
[65] R. Weissleder, H. Lee, J. Ko, M.J. Pittet, COVID-19 diagnostics in context, Sci. Transl. Med. 12 (2020), https://doi.org/10.1126/scitranslmed.abc1931 eabc1931.
[66] L.M. Kucirka, S.A. Lauer, O. Laeyendecker, D. Boon, J. Lessler, Variation in false-negative rate of Reverse Transcriptase polymerase chain reaction–based SARS-CoV-2 tests by time since exposure, Ann. Intern. Med. 173 (2020) 262–267, https://doi.org/10.7326/M20-1495.
[67] G. Lippi, A.-M. Simundic, M. Plebani, Potential preanalytical and analytical vulnerabilities in the laboratory diagnosis of coronavirus disease 2019 (COVID-19), Clin. Chem. Lab. Med. 58 (2020) 1070–1076, https://doi.org/10.1515/cclm-2020-0285.
[68] P.R. Lephart, M.A. Bachman, W. LeBar, S. McClellan, K. Barron, L. Schroeder, D. W. Newton, Comparative study of four SARS-CoV-2 Nucleic Acid Amplification Test (NAAT) platforms demonstrates that ID NOW performance is impaired substantially by patient and specimen type, Diagn, Microbiol. Infect. Dis. 99 (2021), 115200, https://doi.org/10.1016/j.diagmicrobio.2020.115200.
[69] H. Yao, Y. Song, Y. Chen, N. Wu, J. Xu, C. Sun, J. Zhang, T. Weng, Z. Zhang, Z. Wu, L. Cheng, D. Shi, X. Lu, J. Lei, M. Crispin, Y. Shi, L. Li, S. Li, Molecular architecture of the SARS-CoV-2 virus, Cell 183 (2020) 730–738, https://doi.org/10.1016/j.cell.2020.09.018, e13.